IOPscience iopscience.iop.org

Home Search Collections Journals About Contact us My IOPscience

Prediction of superhard cubic boron–carbon nitride through first principles

This article has been downloaded from IOPscience. Please scroll down to see the full text article.

2009 J. Phys.: Condens. Matter 21 415403

(http://iopscience.iop.org/0953-8984/21/41/415403)

View the table of contents for this issue, or go to the journal homepage for more

Download details:
IP Address: 129.252.86.83
The article was downloaded on 30/05/2010 at 05:33

Please note that terms and conditions apply.

J. Phys.: Condens. Matter **21** (2009) 415403 (6pp) doi:10.1088/0953-8984/21/41/415403

Prediction of superhard cubic boron–carbon nitride through first principles

Koretaka Yuge

Department of Materials Science and Engineering, Kyoto University, Sakyo, Kyoto 606-8501, Japan

Received 3 June 2009, in final form 28 August 2009
Published 23 September 2009
Online at stacks.iop.org/JPhysCM/21/415403

Abstract

Superhard cubic boron–carbon nitride (c-BNC) in terms of bulk modulus along a composition range of $(BN)_{(1-x)}(C_2)_x$ $(0 \leqslant x \leqslant 1)$ is systematically explored by Monte Carlo simulations and cluster expansion techniques based on first-principles calculation. Bulk moduli for the c-BNC ordered structures are reasonably expanded up to quadruplet clusters, indicating that dependence of the bulk modulus on atomic arrangements is not simply attributed to pairwise interactions. A negative correlation can be seen between bulk modulus and formation energies, which is consistent with previous theoretical works. Monte Carlo simulation reveals that all the ordered structures with the highest bulk modulus at each composition exhibit a strong preference of neighboring B–N and C–C atoms, which is consistent with the bond counting rule previously suggested. A composition dependence of these ordered structures can be observed. At a BN-rich composition of $x = 0.25$, C atoms form a nearest-neighbor network with a hexagonal cluster shape, while at equiatomic and diamond-rich compositions of $x = 0.5$ and 0.75, B and N atoms form nearest-neighbor networks with a planar shape. At $x = 0.875$, c-BNC ordered structure with neighboring B and N atoms forming a stereoscopic shape exhibit the highest bulk modulus of 459.3 GPa, which is ∼0.6% smaller than that of diamond.

(Some figures in this article are in colour only in the electronic version)

1. Introduction

Alloys of diamond and cubic (c)-BN, cubic BNC (c-BNC), have been promising candidates for new superhard materials and are expected to show high thermal and chemical stability compared with diamond, which are motivated by the similarity of lattice constants, high melting temperature and bulk modulus, and similar thermal expansion coefficients of diamond and c-BN. With these promising potentialities, several syntheses of c-BNC are successfully performed and their physical properties are carefully investigated so far. The synthesized c-BNC exhibits a wide variety of bulk moduli: Solozhenko *et al* [1] synthesized c-BC_2N using hydrostatic compression of ∼30 GPa, which shows a bulk modulus of 282 ± 15 GPa. Tkachev *et al* [2] measured a bulk modulus of 259 ± 22 for the c-BC_2N using Brillouin scattering. The synthesized c-BC_2N for [1] and [2] show significantly smaller bulk moduli than that of c-BN (370–400 GPa) [3]. Meanwhile, Komatsu *et al* [4] obtained c-BC_2N with a bulk modulus of 401 GPa that is larger than that of c-BN. Such c-BCN compounds with high bulk modulus are also synthesized by other investigations: Knittle *et al* [5] synthesized cubic $C_{0.33}(BN)_{0.67}$ under a high pressure of 30–50 GPa and high temperature of 2000–2500 K, which shows bulk moduli of 355 ± 19 GPa.

Theoretical investigations based on density functional theory (DFT) have also been actively carried out in order to identify the c-BNC phase with experimentally observed lower and higher bulk moduli and to search for ordered c-BNC structure with high hardness. Sun *et al* [6] perform a DFT calculation on all seven possible c-BC_2N ordered structures within the unit cell, which show bulk moduli of 290–400 GPa. Zhang *et al* [7] address the hardness of several c-BC_2N ordered structures in terms of compositional anisotropy and strain dependence of bonding character. Pan *et al* [8] reported the possible path of cubic–graphitic transformation and stability of the high density phase for the c-BC_2N, which predict that synthesis of the cubic phase from a graphitic structure can yield high critical tensile strength. Paiva *et al* [9] investigated

 © 2009 IOP Publishing Ltd Printed in the UK

five cubic $(BN)_xC_{2(1-x)}$ $(0 \leqslant x \leqslant 1)$ ordered structures and show that composition dependence of bulk moduli ranging from 370–400 GPa exhibit negative deviation from the linear average of c-BN and diamond. Guo *et al* [10] estimated the Vickers hardness for four selected configuration of c-BC_2N in the unit cell and predicted that c-BC_2N can be the second-hardest material instead of c-BN. Chen *et al* [11] predicted c-BC_2N with higher bulk moduli of 400–420 GPa based on the bond counting rule [12], where the structures are characterized by a short period (111) superlattice. Zhou *et al* [13] also predict superhard c-BC_2N with a 16-atom cell, where the bulk modulus is estimated to be ∼402.7 GPa.

These previous studies certainly give us a wide variety of important information about the relationship between the hardness of c-BC_2N and chemical bonding or atomic arrangements. However, in terms of designing superhard c-BC_2N materials through *ab initio* calculations, there still remains a good possibility that a new superhard c-BC_2N ordered structure can be found. This is because, in the previous studies, (i) the model structures for the c-BCN are somehow constructed artificially or are preliminary confined to specific atomic arrangements, (ii) the number of structures that were considered are extremely small (within a few tens of structures), while even $2 \times 2 \times 2$ expansion of the diamond unit cell with B, C and N atoms results in 3^{64} structures, which is an astronomical number and (iii) the composition investigated is mostly confined to BC_2N in order to compare with those measured such as high and low density phases.

With these considerations, further investigation is required in order to comprehensively search the potentialities for superhard c-BCN alloys. In the present work, the hardness of the c-BNC alloy is examined in terms of the bulk modulus in the composition range of $(BN)_{(1-x)}(C_2)_x$ $(0 \leqslant x \leqslant 1)$, which has naturally led from the mixture of c-BN and diamond. Note that, although the bulk modulus, B_0, does not necessarily correspond to the practical hardness of the material [7], it certainly reflects the ideal hardness near equilibrium positions under isotropic compression. In order to systematically and effectively search superhard c-BNC ordered structures, we employ the cluster expansion [14, 15] (CE) technique based on the DFT total energy calculations. A definite advantage in using the CE is that (i) by using the limited number of DFT calculations for B_0, the CE can powerfully predict B_0 for millions of c-BNC ordered structures with desirable accuracy and (ii) the DFT input structures are self-consistently selected, and not by hand, so that atomic arrangements of c-BNC with higher B_0 are effectively predicted. The details of the present calculation is described in the following sections.

2. Methodology

2.1. Cluster expansion technique

Since the bulk modulus B_0 is a function of atomic arrangement $\vec{\sigma}$ and composition, the CE technique can be applied to expand B_0. The essence of the CE is an expansion of any property (here, B_0) in terms of the atomic arrangements. In this technique, we first introduce the variables $\sigma_i = \{+1, 0, -1\}$ that specify the occupation of B, C and N atoms at lattice point i on a heterodiamond structure. Using σ_i, we can construct functions that are complete and orthonormal for the whole N lattice points in the given system [16]:

$$\begin{aligned} B_0(\vec{\sigma}) &= V_0\Phi_0 + \sum_n \sum_{(\tau)} V_n^{(\tau)} \Phi_n^{(\tau)}(\vec{\sigma}) \\ \Phi_n^{(\tau)} &= \prod_{\substack{i\in n \\ d\in(\tau)}} \phi_d(\sigma_i) \qquad \phi_0(\sigma_i) = 1 \\ \phi_1(\sigma_i) &= \sqrt{\tfrac{3}{2}}\sigma_i \qquad \phi_2(\sigma_i) = -\sqrt{2}(1 - \tfrac{3}{2}\sigma_i^2), \end{aligned} \tag{1}$$

where the expansion coefficient V is typically called an effective cluster interaction (ECI) that is independent of $\vec{\sigma}$, $\phi(\sigma_i)$ is the orthonormal basis function at lattice point i and Φ is called the cluster function obtained by products of ϕs. n specifies the set of lattice points whose basis function is not unity (i.e. $\neq\phi_0$), which corresponds to the cluster figure. (τ) specifies the set of basis-function indexes described by the subscript of ϕ.

In order to determine the ECIs, we perform least-squares (LS) fitting of the B_0 for c-BNC ordered structures obtained via DFT calculations. B_0 is estimated by applying the finite compression or expansion of volume to the geometry-optimized cell [20]. For DFT calculations on c-BNC under compression or expansion, geometry optimization is performed with constant volume. We obtain B_0 for 255 ordered structures, each of which consists of 64 atoms, i.e. a $2 \times 2 \times 2$ expansion of the unit cell in the diamond structure. Other DFT calculation conditions are described elsewhere [16, 17]. Due to the limitation number of DFT calculations, the expansion in equation (1) should be truncated at finite order. Therefore, we should choose an optimal set of clusters $\{n\}$ that give accurate prediction of bulk modulus for given atomic arrangements. An optimal set of clusters are chosen using the genetic algorithm [18, 19] to minimize the uncertainty of B_0 predicted by ECIs, called a cross-validation (CV) score [22, 23]. An optimal set of DFT input structures is chosen in a similar way to choosing energetically favorable structures based on the construction of a ground-state diagram [21]: (i) B_0 for randomly selected ordered structures are estimated via DFT calculation, which are then applied to a genetic algorithm to obtain an optimal set of clusters and their ECIs. (ii) B_0 for all possible atomic arrangements and compositions are comprehensively estimated using the resultant ECIs. (iii) For each composition, when ordered structures with higher bulk modulus are not included in the DFT calculations, B_0 for these structures are estimated via DFT calculation. The procedure (i)–(iii) is repeated until the CE prediction in (iii) becomes consistent in the DFT calculation.

2.2. Monte Carlo simulation

Since for the ternary $(BN)_{(1-x)}(C_2)_x$ $(0 \leqslant x \leqslant 1)$ system, even a $2 \times 2 \times 2$ expansion of the diamond unit cell have a astronomical number of possible atomic arrangements, estimation of B_0 for all these arrangements is not practical. In the present work, we perform MC simulation with a

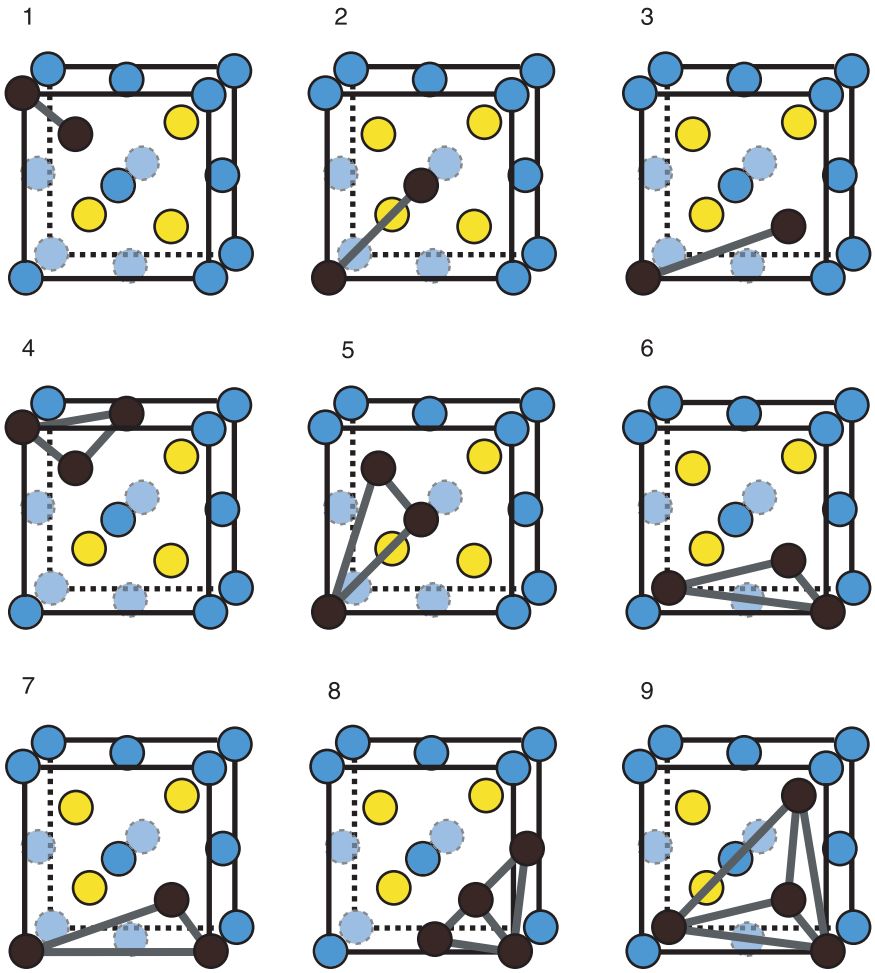

Figure 1. Selected multibody clusters used in the expansion of bulk modulus for c-BNC ordered structures. Tetrahedral and fcc sites are illustrated by yellow and blue spheres (or faint color in the monochrome image). Black (or dark) spheres connected with bold lines denote used clusters.

simulated algorithm in order to effectively sweep across the representative and highest B_0 among possible atomic arrangements. In the MC, the flipping probability from old state i to new state j is given by

$$P_{i\to j} = \exp\left(-\frac{\Delta B}{k_{\mathrm{B}}T}\right), \tag{2}$$

where ΔB denotes the bulk modulus for a new state measured from that for the old state and T corresponds to the temperature for conventional MC simulation under a canonical ensemble. We perform MC simulation using a $2 \times 2 \times 2$ expansion of a diamond unit cell under three-dimensional periodic boundary conditions. Initial temperature of the MC simulation box is at $T = 1000$ K, and is gradually decreased by 5 K after 10 000 Monte Carlo steps per site until the temperature becomes 0 K. During the simulation, all the B_0 for each MC step are recorded.

3. Results and discussion

3.1. Effective cluster interactions for c-BNC ternary system

Following the procedure in section 2, we finally choose 11 clusters consisting of one empty, one point, three pair, four triplet and two quadruplet clusters; multibody clusters are shown in figure 1. These multibody clusters all consist of up to eighth-nearest-neighbor pairs. The set of clusters shows a CV score of 0.7 GPa, where the standard deviation of the DFT fitted bulk modulus is 55.4 GPa. These clusters give sufficient accuracy for expressing relative B_0 of individual atomic arrangements in the c-BNC. Figure 2 shows the corresponding ECIs. We can see that ECIs for the triplet and quadruplet clusters are of the same order as those for the pair clusters, which is in contrast to the expansion of c-BNC total energies where ECIs for pair clusters, particularly along first-nearest-neighbor (1-NN) coordination, possess dominant contribution [16, 17]. This fact certainly indicates that the dependence of bulk modulus on atomic arrangements is not simply attributed to the pairwise interactions.

3.2. Bulk modulus for c-BNC

We first show in figure 3 the bulk modulus obtained via DFT calculation as a function of formation energy. Here, the formation energy of E_{form} is defined as

$$E_{\mathrm{form}}(\vec{\sigma}) = E(\vec{\sigma}) - (1-x)E_{\mathrm{c-BN}} - 2xE_{\mathrm{diamond}}, \tag{3}$$

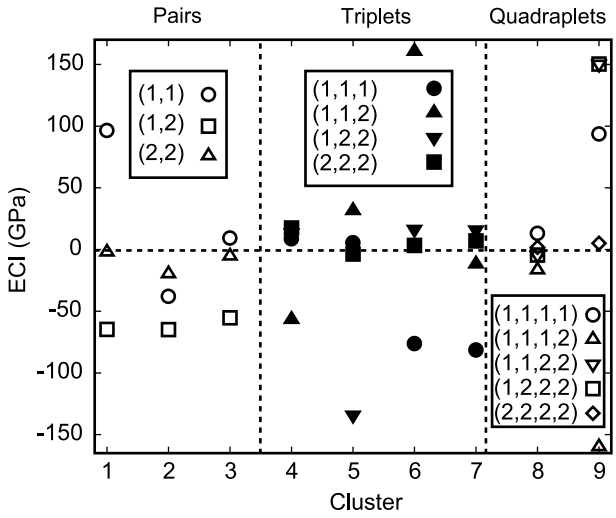

Figure 2. Effective cluster interactions for the multibody clusters in c-BNC. Parentheses denote basis functions for each lattice point given by equation (1).

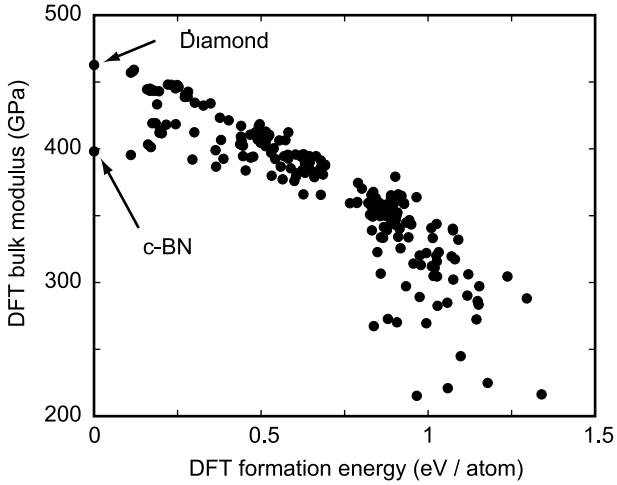

Figure 3. Bulk modulus B_0 for ordered structures obtained via DFT calculation as a function of DFT formation energies defined in equation (3).

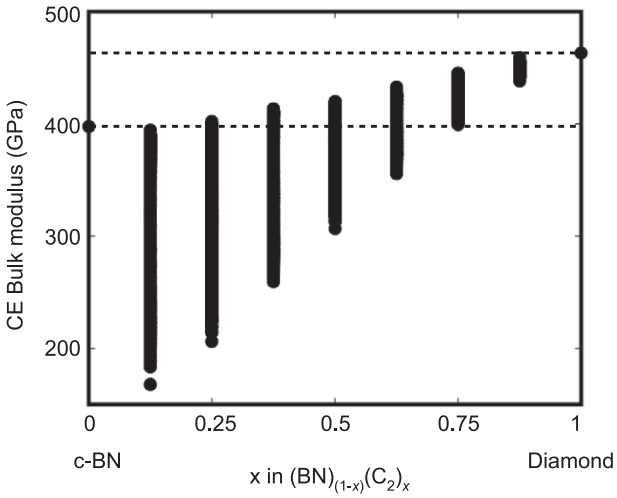

Figure 4. Cluster expansion prediction of bulk modulus B_0 for possible ordered c-BNC structures as a function of composition x.

where $E(\vec{\sigma})$ denotes total energy of the c-BNC ordered structure in a composition of $(BN)_{(1-x)}(C_2)_x$, and E_{c-BN} and $E_{diamond}$ denote total energy of c-BN and diamond in the formula unit, respectively. Calculated B_0 for diamond and c-BN are estimated to be 462 and 397 GPa, which are in satisfactory agreement with the measured B_0 of 443 GPa [5, 24] and 369 ± 14 GPa [25]. Slightly higher bulk moduli of both diamond and c-BN in the present calculation are due to zero-temperature calculation where thermal expansion is neglected and to the LDA approximation to the exchange–correlation functional which typically underestimates lattice constants, resulting in overestimation of B_0. It is clear from figure 3 that there is certainly a negative correlation between bulk modulus and formation energy: structures with lower formation energies tend to have a higher bulk modulus, which is consistent with previous theoretical predictions [12, 13]. This can be partially attributed to the fact that the formation of energetically stable neighboring B–N bonds decrease the volume of the c-BNC alloy [17, 26], which would lead to an increase in bulk modulus. All the structures exhibit positive formation energies, indicating no stable c-BNC ordered structures with high bulk modulus exists between diamond and c-BN.

A comprehensive search of bulk modulus with respect to composition x can be performed by applying ECIs in figure 2 to the MC simulation with a simulated annealing algorithm described in section 2. Figure 4 shows the resultant bulk modulus for the representative ordered structures as a function of composition x whose grid is set at 0.125. Horizontal dotted lines correspond to the bulk modulus of c-BN and diamond. Several important features can be seen from figure 4: (i) there exists several ordered structures that exhibit higher bulk modulus than that of the c-BN for a composition range of $x \geqslant 0.25$. (ii) With an increase of composition x, bulk moduli for ordered structures with highest and lowest B_0 both increase. (iii) At $x = 0.825$, an ordered structure with the highest B_0 is found where B_0 is slightly lower than that of diamond. (iv) Dispersion of the bulk modulus get larger with the decrease in x, which will be discussed later.

In order to see the actual atomic arrangements that possess higher bulk moduli in figure 4, we illustrate in figure 5 the ordered structures that exhibit the highest or second-highest bulk modulus at $x = 0.25$, 0.5, 0.75 and 0.825. Black spheres denote C atoms, and green and white spheres denote B and N atoms, respectively. In figure 5, neighboring C–C or B–N bonds are illustrated together in order to make intuitively clear the atomic arrangements. We can clearly see that structural character for highest bulk modulus certainly depends on concentration. At $x = 0.5$ and 0.75 for BNC_2-1, BNC_6-1 and BNC_6-2, they have a characteristic nearest-neighbor B–N network along the (111) plane: BNC_2-1 at $x = 0.5$ has alternate stacking of neighboring B–N and C–C networks with the (111) plane similar to $L1_1$ ordering in CuPt alloy. BNC_6-1 and BNC_6-2 at $x = 0.75$ have neighboring B–N networks in single or a combination of planar shapes

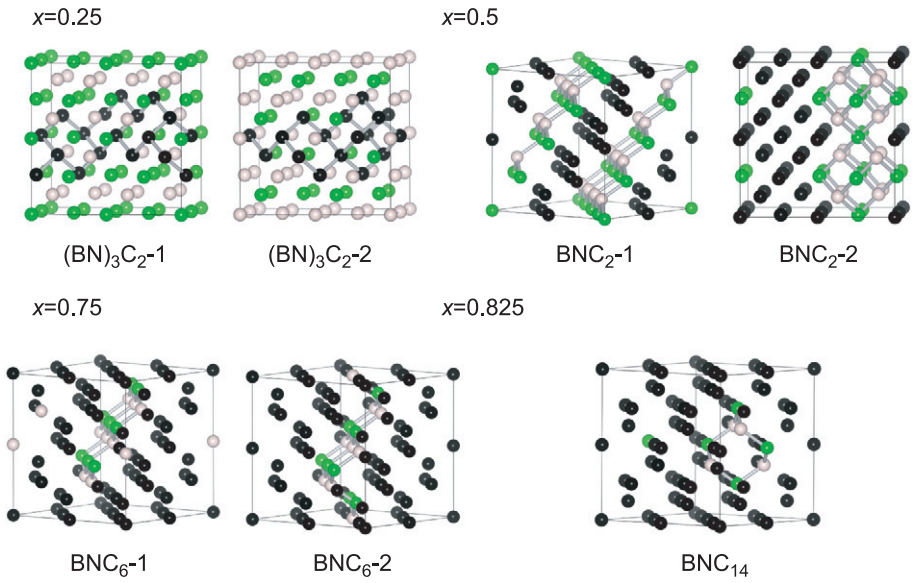

Figure 5. Predicted c-BNC ordered structures that exhibit highest or second-highest bulk modulus at $x = 0.25$, 0.5, 0.75 and 0.825. Black, green (or gray in the monochrome image) and white spheres denote C, B and N atoms, respectively.

Table 1. Bulk modulus B_0, volume for 64-atom cell, and affinity α defined in equation (4) along 1-NN coordination. Brackets in the volume V column denote deviation from the linear-average volume of c-BN and diamond (i.e. Vegard's law).

				Affinity					
x	Structure	B_0 (GPa)	V (Å^3)	α_{BB}	α_{CC}	α_{NN}	α_{BC}	α_{BN}	α_{CN}
0.25	$(BN)_3C_2$-1	403.3	367.21 (+0.7%)	−1.00	1.50	−1.00	−0.50	1.33	−0.50
	$(BN)_3C_2$-2	401.3	367.21 (+0.7%)	−1.00	1.50	−1.00	−0.50	1.33	−0.50
0.5	BNC_2-1	419.2	364.25 (+0.9%)	−1.00	0.50	−1.00	−0.50	2.00	−0.50
	BNC_2-2	418.4	364.13 (+0.8%)	−1.00	0.50	−1.00	−0.50	2.00	−0.50
0.75	BNC_6-1	443.9	359.83 (+0.6%)	−1.00	0.15	−1.00	−0.46	3.75	−0.46
	BNC_6-2	444.9	359.67 (+0.6%)	−1.00	0.17	−1.00	−0.50	4.00	−0.50
0.825	BNC_{14}	459.3	357.05 (+0.2%)	−1.00	0.06	−1.00	−0.43	7.00	−0.43

that have an interface of the (111) plane with C atoms. In particular, the BNC_2-1 structure at $x = 0.5$ is consistent with the $BC_2N_{1\times1}$ structure theoretically modeled by Chen *et al* [26] which is predicted to be the synthesized high density c-BNC phase containing large amounts of (111) superlattices. For BNC_2-2 at $x = 0.5$, the structure seems phase separating in a finite cell with its interface between diamond and c-BN consisting of the (110) plane. For the BNC_{14} at $x = 0.825$ with the highest bulk modulus, B and N atoms form a nearest-neighbor network with stereoscopic shape, not with a planar shape. At $x = 0.25$ for $(BN)_3C_2$-1 and-2, C atoms form a nearest-neighbor network with cluster-like shape that consists of six-atom hexagons, each of which share sides or vertices. In order to quantitatively see which elemental bonds are preferred in ordered structures with high bulk modulus, we introduce the affinity α defined as

$$\alpha_{IJ} = \frac{y_{IJ}(\text{system})}{y_{IJ}(\text{random})} - 1, \tag{4}$$

where y_{IJ}(system) and y_{IJ}(random) represent the pair probability of I–J elements for the system and completely disordered alloy, respectively. Therefore, $\alpha_{IJ} > 0$ represents a preference of I–J bonds and $\alpha_{IJ} < 0$ a lack of preference. Note that from the definition of the affinity of equation (4), the lower limit of α is -1, while the upper limit depends on the system.

Table 1 summarizes predicted bulk modulus, volume for 64-atom cell and affinity α defined in equation (4) along a 1-NN coordination for ordered structures illustrated in figure 5. The volumes for all the structures exhibit slightly positive deviation (0.2–0.7%) from Vegard's law, which agrees with a positive deviation of 0.5–1.1% for synthesized $(BN)_xC_{(1-x)}$ ($x = 0.3$–0.33, 0.5, 0.6) solid solution with high bulk modulus of 355 ± 19 GPa [5]. All the ordered structures with highest bulk modulus exhibit positive affinity for B–N and C–C bonds along 1-NN coordination. As a counterpart, the affinity for other bonds show a negative value: affinities for B–B and N–N bonds are -1, while those for B–C and C–N bonds show a negative but larger than -1 value. This can explain the dependence of dispersion in the bulk modulus on composition x in figure 4: c-BNC ordered structures with high bulk modulus prefer neighboring B–N and C–C bonds while strongly disfavoring B–B and N–N bonds. At smaller x, there can be a wide variety of atomic arrangements with a large number of B–B and N–N bonds or a large number of B–N bonds due to a large number of B and N atoms, which naturally

result in a larger dispersion in bulk modulus. Meanwhile, at larger x, due to a decrease in the number of B and N atoms, the number of ordered structures with lower bulk modulus should significantly decrease, leading to a decrease of dispersion in the bulk modulus. The tendency of the affinity also holds for energetically favored c-BNC ordered structures which strongly favor neighboring B–N and C–C bonds while disfavoring B–B and N–N bonds [16]. Therefore, energetically favored ordered structures tend to exhibit higher bulk modulus, which can also be seen in figure 3. Moreover, formation of neighboring B–N and C–C bonds tend to decrease the volume of the c-BNC ordered structures [17], which would also contribute to an increase in bulk modulus. The tendency of affinities to increase in bulk modulus agrees with the previously proposed bond counting rule, where energetically favored neighboring B–N and C–C bonds tend to increase the hardness of the c-BNC [12, 13]. However, such a rule is clearly not sufficient to explain the composition dependence of the B–N or C–C bond network, as shown in figure 5. Bulk modulus for the c-BNC is not simply attributed to pairwise but to multibody interactions as shown in figure 2, which indicates that the present comprehensive and automatic study can be an effective and widely applicable approach to the design of superhard materials based on *ab initio* calculations. Since the predicted ordered structures at $x \geqslant 0.75$ with higher bulk modulus than those at $x = 0.5$ have not been reported so far, these results could significantly contribute to the experimental trial to synthesize the superhard c-BNC by experimental work.

4. Conclusions

Superhard cubic boron–carbon nitride (c-BNC) in the composition range of $(BN)_{(1-x)}(C_2)_x$ $(0 \leqslant x \leqslant 1)$ is systematically investigated by a combination of Monte Carlo simulations and cluster expansion techniques based on the first-principles calculation. ECIs for quadruplet clusters in the expansion of the bulk modulus are of the same order as those for pair clusters, indicating that dependence of the bulk modulus on atomic arrangements is not simply attributed to pairwise interactions. Negative correlation can be seen between the bulk modulus and formation energies, which is consistent with previous theoretical works. MC simulation with a simulated annealing algorithm reveal that all the ordered structures with highest bulk modulus at each composition exhibit a strong preference of neighboring B–N and C–C atoms, which is consistent with the bond counting rule previously suggested. Formation of the neighboring B–N and C–C atoms is energetically preferred and also decrease the volume of the c-BNC solid solution, which would contribute to increasing the bulk modulus. Composition dependence of atomic arrangements with the highest bulk modulus can be seen: at a BN-rich composition of $x = 0.25$, C atoms form a nearest-neighbor network with a hexagonal cluster shape, while at equiatomic and diamond-rich compositions of $x = 0.5$ and 0.75, B and N atoms form a nearest-neighbor network with a planar shape. At $x = 0.5$, predicted ordered structure is consistent with a theoretically modeled $BC_2N_{1\times1}$ structure, which is predicted to be the synthesized high density c-BNC phase containing a large amount of (111) superlattices. For other compositions of $x \geqslant 0.25$, we have found several ordered structures with higher bulk modulus than that of c-BN. Since the predicted ordered structures have not been reported so far, the present results contribute to an experimental trial to synthesize such superhard c-BNC.

Acknowledgment

The author would like to express cordial thanks to Dr Fumiyasu Oba of Kyoto University for fruitful suggestions in this work.

References

[1] Solozhenko V L, Andrault D, Fiquet G, Mezouar M and Rubie D C 2001 *Appl. Phys. Lett.* **78** 1385
[2] Trachev S N, Solozhenko V L, Zinin P V, Manghnani M H and Ming L C 2003 *Phys. Rev.* B **68** 052104
[3] Janotti A, Wei S-H and Singh D J 2001 *Phys. Rev.* B **64** 174107
[4] Komatsu Y, Nomura M, Kakudate Y and Fujisawa S 1996 *J. Mater. Chem.* **6** 1799
[5] Knittle E, Kaner R B, Jeanloz R and Cohen M L 1995 *Phys. Rev.* B **51** 12149
[6] Sun H, Jhi S-H, Roundy D, Cohen M L and Louie S G 2001 *Phys. Rev.* B **64** 094108
[7] Zhang Y, Sun H and Chen C 2004 *Phys. Rev. Lett.* **93** 195504
[8] Pan Z, Sun H and Chen C 2006 *Phys. Rev.* B **73** 214111
[9] de Paiva R and Azevedo S 2006 *J. Phys.: Condens. Matter* **18** 3509
[10] Guo X, Liu Z, Luo X, Yu D, He J, Tian Y, Sun J and Wang H-T 2007 *Diamond Relat. Mater.* **16** 526
[11] Chen S, Gong X G and Wei S-H 2007 *Phys. Rev. Lett.* **98** 015502
[12] Tateyama Y, Ogitsu T, Kusakabe K, Tsuneyuki S and Itoh S 1997 *Phys. Rev.* B **55** R10161
[13] Zhou X-F, Sun J, Fan Y-X, Chen J, Wang H-T, Guo X, He J and Tian Y 2007 *Phys. Rev.* B **76** 100101
[14] Sanchez J M, Ducastelle F and Gratias D 1984 *Physica* A **128** 334
[15] de Fountain D 1994 *Solid State Physics* vol 47, ed H Ehrenreich and D Turnbull (Cambridge, MA: Academic) pp 33–176
[16] Yuge K, Seko A, Koyama Y, Oba F and Tanaka I 2008 *Phys. Rev.* B **77** 094121
[17] Yuge K 2009 *J. Phys.: Condens. Matter* **21** 055403
[18] Hart G L W, Blum V, Walorski M J and Zunger A 2005 *Nat. Mater.* **4** 391
[19] van de Walle A 2005 *Nat. Mater.* **4** 362
[20] Yuge K, Seko A, Kobayashi K, Tatsuoka T, Nishitani S R and Adachi H 2004 *Mater. Trans.* **45** 1473
[21] Blum V and Zunger A 2004 *Phys. Rev.* B **70** 155108
[22] Stone M 1974 *J. R. Stat. Soc. Ser.* B **36** 111
[23] Allen D M 1974 *Technometrics* **16** 125
[24] Yin M T 1984 *Phys. Rev.* B **30** 1773
[25] Knittle E, Wentzcovitch R M, Jeanloz R and Cohen M L 1989 *Nature* **337** 349
[26] Chen S, Gong X G and Wei S-H 2008 *Phys. Rev.* B **77** 014113